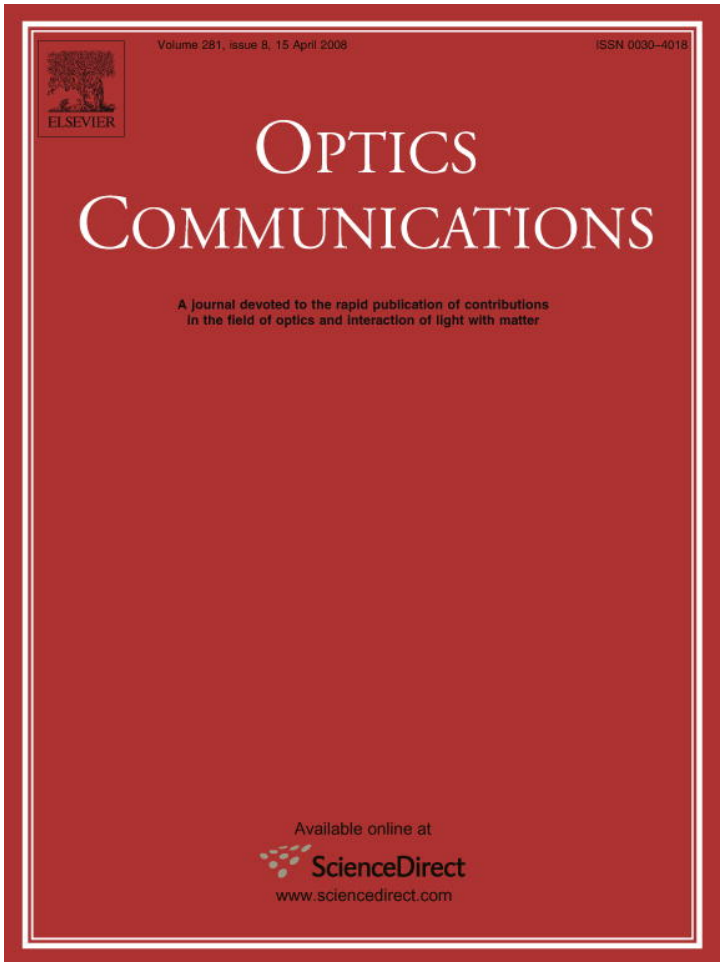

Available online at www.sciencedirect.com
ScienceDirect
Optics Communications 281 (2008) 1915–1923
OPTICS COMMUNICATIONS
www.elsevier.com/locate/optcom

Automatic fringe analysis of the induced anisotropy of bent optical fibres

T.Z.N. Sokkar [a], M.A. El-Morsy [b,*], H.H. Wahba [b]

[a] Department of Physics, Faculty of Science, University of Mansoura, Mansoura, Egypt
[b] Department of Physics, Faculty of Science, University of Mansoura, New Damietta, Egypt

Received 5 July 2007; received in revised form 13 November 2007; accepted 23 November 2007

Abstract

A new theoretical model considering the refraction of the incident light beam by the fibre is suggested to determine the refractive index profile of bent optical fibres. This new model (slabs model) considering the cross section of the bent optical fibre consists of large number of slabs. The slabs model bases on the refraction of the incident beam by the fibre. The refractive index profile of the optical fibre cladding before bending obtained using the automated Fizeau interferometer with the aid of suggested model is compared with other models such as, the homogenous model and the multilayer model to verify the ability of this slab model. The refractive index profile of the bent optical fibre cladding is investigated using this suggested model. In addition, the new model is used to obtain the induced birefringence and the guiding parameters. The bending radius is recommended to be greater than 7.1 mm for the used optical fibre. The consideration of the refraction increases the accuracy of the results.

Keywords: Optical fibre; Refractive index profile; Induced birefringence; Fizeau interferometer

1. Introduction

The optical fibre is a dielectric waveguide [1] structure that transports energy at optical frequencies. Generally, the optical fibre consists of a core surrounded by a cladding. Two common types of multimode optical fibres are step index fibres and graded index fibres. As well as the single mode, optical fibres are used widely in the long distance communications. Cylindrical fibres of circular cross section are most common fibre geometries. The refractive index profile and the material dispersion have strong effect on the group delay characteristics of an optical fibre. Therefore, the refractive index profile of optical fibre is important not only in assessing the performance of the fibre in a given system but also it helps in fibre fabrication [2] to improve its products.

Many authors have studied the refractive index measurements using interferometric methods [3–11]. Some authors determined the influence of temperature on the refractive index profile of fibres [12].

Hibino et al. [13] studied the effect of the mechanically induced residual stress on the refractive index of the single mode optical fibre. The birefringence was being negative for the elongation stress.

The isotropic plastic optical fibre becomes a uniaxial fibre as a result of bending effect. The induced birefringence is proportional to the distance measured from the neutral line [14]. Tai et al. [15] gave more generalized study which applicable for all plastic and glass fibres, they observed that, the bending leads to increase of refractive index in compression part and vice versa. The macro bending loss for optical fibres was studied as a function of the bending radius using the beam propagating method [16,17].

The relation between the induced birefringence and the mechanical strain is described for the bent fibre cladding [18].

* Corresponding author. Tel.: +20 572403980; fax: +20 572403868.
E-mail address: elmorsym@yahoo.com (M.A. El-Morsy).

0030-4018/$ - see front matter © 2007 Elsevier B.V. All rights reserved.
doi:10.1016/j.optcom.2007.11.094

The refractive index profile of an optical fibre influenced by the stresses caused by pure bending and an induced birefringence was observed [19]. El-Diasty calculated the asymmetrical refractive index profile and induced birefringence for the bent single mode optical fibre cladding using the Fizeau interferometer in transmission [19]. The mathematical expressions used in the calculations [19] of the bent optical fibre parameters neglected the refraction of the incident light beam by the bent optical fibre.

Different optical techniques have been developed to determine the fibre refractive index profile. The advantage of optical techniques over the other techniques is that it can provide whole field information for analysis. They usually produce contour maps in terms of fringe pattern, which can be used for investigating systems quickly and easily by visual inspection [20].

The multiple-beam Fizeau fringe system is a sensitive optical technique for measuring the optical properties of optical fibre and gives accurate results due to the sharpness of the interference fringe, compared with two-beam interference fringe.

Multiple-beam Fizeau fringes are formed across the fibre when immersed in a silvered liquid wedge interferometer illuminated by a parallel beam of polarized monochromatic light. The shift in the position of the interference fringe is formed because the fibre inside the interferometer works as a phase object. The optical properties of the fibre are usually encoded into deformed fringe pattern. Thus by observing the fringe shift inside the fibre, the quantitative information about the optical properties of the fibre under test and its structural parameters can be measured. The method in which matching immersion liquids are used to give good results of the fibre refractive index profile, especially when liquid and fibre cladding have refractive indices close to each other. However, to minimize the error in the measured data, it is essential to take into consideration the effect of refraction [8,21] of the beam through the liquid–fibre and core-cladding interfaces.

The focus in this paper is divided into two main points in order to measure the change of refractive index and the related induced birefringence in the cladding of the optical fibre due to bending. The first point is automatically analyzing the multiple-beam Fizeau fringe pattern using Fourier transform fringe analysis technique. The second point is to suggest an accurate new mathematical model for optical path difference in which the refraction of the beam through the fibre due to refractive index change along its radius is considered.

2. Theoretical considerations of the slabs model

Of course, multiple-beam Fizeau interferometry is not the only method of obtaining high special precision but today the multiple-beam Fizeau interferometry is still one of the most compact and highest resolving power interferometer.

The isotropic optical fibre material becomes anisotropic under the effect of the mechanical bending. The induced anisotropy in the bent optical fibre leads to the appearance of optical birefringence. The optical anisotropy of materials can be achieved under the effect of the mechanical stresses [22].

The polarization state of the incident beam will be split into two linear orthogonal components of polarization directions where these directions are parallel and perpendicular to the fibre optical axis. The corresponding refractive indices are $n^{\parallel}$ and $n^{\perp}$. The parallel component of refractive index ($n^{\parallel}$) will be affected with the mechanical bending and the other component still constant ($n^{\perp}$) [19]. The fibre under the bending can be classified into two regions about the neutral plane. The inner region is compressed and the outer region is extended. The refractive index $n^{\parallel}$ of the bent cladding is decreased as x increase and vice versa. Where x is a distance measured from the fibre origin along x-axis. It will be positive in the tension region and negative in the compression region. To determine the refractive index profile of the clad of bent optical fibre we suggest a new model. In this model, we divide the cross section of the bent cladding into Q-thin slabs having refractive indices n_j. These slabs are perpendicular to the bending radius R as shown in Fig. 1. The first slab at the fibre bored and the slab order increase toward its centre. The slab thickness a can be calculated using the following equation;

$$a = \frac{r - r_c}{Q} \tag{1}$$

where r, r_c are the fibre and the core radii respectively.

The bent optical fibre is immersed in a suitable liquid of refractive index n_L in the Fizeau interferometer. The refractive index of the immersion liquid is equal to the perpendicular component of refractive index of the bent optical fibre cladding ($n_L = n^{\perp}$). When putting a bent optical fibre into the object plane of a transmitting Fizeau interferometer, a deviation of the fibre fringe obtained due to the optical path difference between the bent optical fibre material and the surrounding media. Thus, the calculation of optical path difference plays an important rule in the accurate

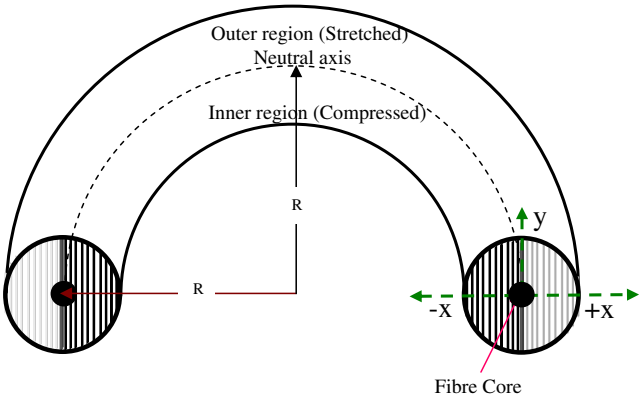

Fig. 1. The schematic diagram of the bent optical fibre.

determination of the refractive index and the other optical properties of fibre.

Now we derive a mathematical expression of the optical path difference in case of taking the refraction of light beam inside the fibre into consideration.

The refractive indices ($n^{\|}$) of the fibre slabs are different from each other. The refractive index of any slab depends on its position along the bent optical fibre diameter. If the bent optical fibre divided into large number of slabs, one can consider the refractive index of a slab number j as n_j.

The refracted beam inside the fibre may pass through one or more slabs. Their paths depend on the refractive index of slabs and the immersion liquid as well as thickness of the slabs. Now we study different cases, when the incident beam pass through one, two, three and kth slabs.

2.1. The refraction through one slab

The first case, when the beam passes only through one slab. Considering the incident beam strikes the slab number j and emerges the fibre from this slab. Fig. 2 shows a schematic diagram for the cross section of the bent optical fibre where the incident beam refracts through one slab. The incident and refraction angles θ_{ij}, θ_{rj} are given by:

$$\theta_{ij} = \sin^{-1}\left(\frac{x_{ij}}{r}\right) \tag{2}$$

$$\theta_{rj} = \sin^{-1}\left(\frac{n_L x_{ij}}{n_j r}\right), \tag{3}$$

where the incident beam strike the slab number j at distance x_{ij} measured from the fibre centre. If the beam traverses the slab j at its centre, the distance x_{ij} can be given from the following equation:

$$x_{ij} = r - (j - 1/2)a \tag{4}$$

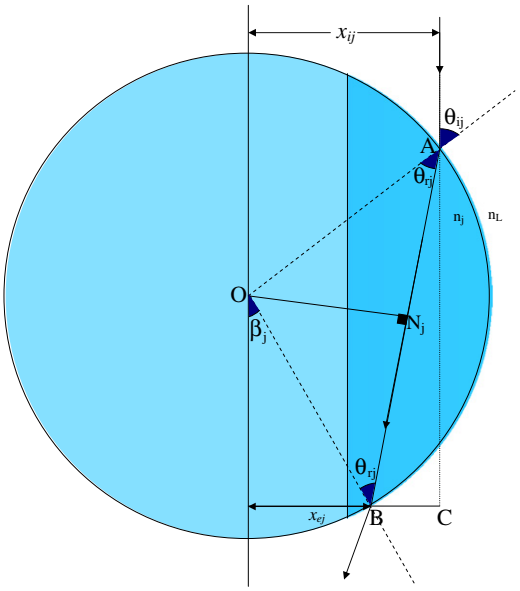

Fig. 2. The ray tracing across the slab number j taking into consideration its refraction inside the fibre.

The refracted beam emerges the fibre at distance x_{ej}, which is expressed as:

$$x_{ej} = r \sin \beta_j \tag{5}$$

where

$$\beta_j = 2\theta_{rj} - \theta_{ij} \tag{6}$$

The optical path difference (OPD) due to the refraction through the slab number j will be given from the following equation;

$$\mathrm{OPD} = n_j \frac{x_{ij} - x_{ej}}{\sin(\theta_{ij} - \theta_{rj})} - n_L \frac{x_{ij} - x_{ej}}{\tan(\theta_{ij} - \theta_{rj})} \tag{7}$$

When using multiple-beam Fizeau interferometer in transmission, one obtains sharp bright fringes on a dark background of interfering spacing h. A monochromatic polarized light of wavelength λ is used. The incident beam will suffer a shift z due to its path through the fibre slab. The optical path difference (OPD) relates to the shift Z_j (after transforming the origin), the wavelength and the interfering spacing by the famous relation (cf. Barakat and Hamza [6]):

$$\mathrm{OPD} = \frac{\lambda Z_j}{2h} \tag{8}$$

Then, Eq. (7) can be rewritten as follows:

$$\frac{\lambda Z_j}{2h} = n_j \frac{x_{ij} - x_{ej}}{\sin(\theta_{ij} - \theta_{rj})} - n_L \frac{x_{ij} - x_{ej}}{\tan(\theta_{ij} - \theta_{rj})} \tag{9}$$

This equation is derived considering the refraction of the incident beam through one slab only.

2.2. The refraction through two slabs

When the incident beam passes through two slabs, the beam will enter the fibre at the slab number j and leave the fibre from the slab number $j+1$ as shown in Fig. 3. The incidence and refraction angles for the slab number j are given by Eqs. (2) and (3). Using the geometry of Fig. 3 we can get:

$$\theta_{ij+1} = \frac{\pi}{2} - (\theta_{ij} - \theta_{rj}) \tag{10}$$

where, θ_{ij+1} is the incidence angle to the slab number $j+1$.

The refraction angle θ_{rj+1} at the slab number $j+1$ is expressed as:

$$\theta_{rj+1} = \sin^{-1}\left[\frac{n_j}{n_{j+1}} \cos(\theta_{ij} - \theta_{rj})\right] \tag{11}$$

The beam will leave the fibre from the slab number $j+1$ at distance x_{ej+1}, which measured from the fibre centre and is given by:

$$x_{ej+1} = r \sin \beta_{j+1} \tag{12}$$

where

$$\beta_{j+1} = (\theta_{ej+1} + \theta_{rj+1}) - \frac{\pi}{2} \tag{13}$$

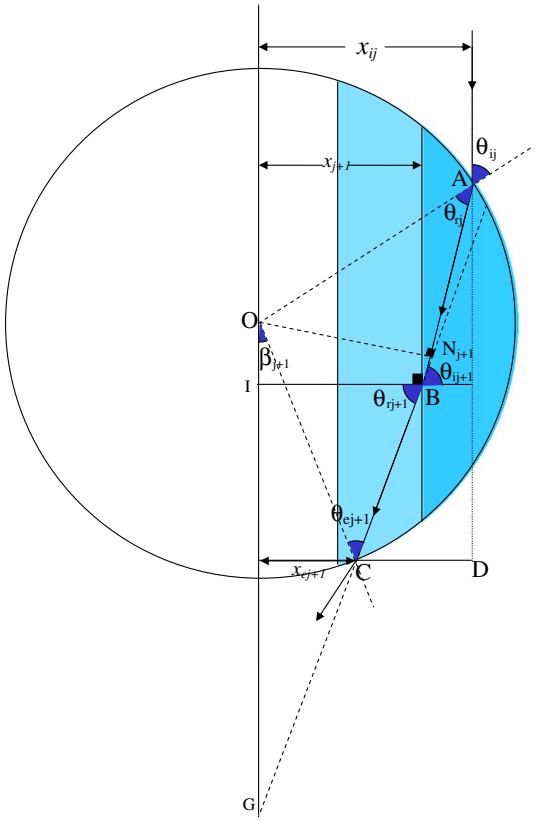

Fig. 3. The ray tracing across two slabs j, $j+1$.

The incident angle at the interface between the slab $j+1$ and the immersion liquid is calculated using the following equation:

$$\theta_{ej+1} = \sin^{-1}\left(\frac{\mathrm{ON}_{j+1}}{r}\right) \tag{14}$$

The distance from the fibre centre to the edge of the slab $j+1$ is x_{j+1} and is given by:

$$x_{j+1} = r - ja \tag{15}$$

The optical path difference in this case can be written in the following form:

$$\frac{\lambda Z_{jj+1}}{2h} = \left[n_j \frac{x_{ij} - x_{j+1}}{\sin(\theta_{ij} - \theta_{rj})} + n_{j+1} \frac{x_{j+1} - x_{ej+1}}{\cos(\theta_{rj+1})}\right] - n_{\mathrm{L}}\left[\frac{x_{ij} - x_{j+1}}{\tan(\theta_{ij} - \theta_{rj})} + [(x_{j+1} - x_{ej+1})\tan\theta_{rj+1}]\right] \tag{16}$$

where Z_{jj+1} is the resultant shift due to the refraction of the incident beam through two slabs j and $j+1$.

2.3. The refraction through three slabs

When the beam refracted through three slabs (j, $j+1$ and $j+2$) where the incident beam entering the fibre at slab j and exit from the slab $j+2$. The angles of incidence and refraction will be given from Eqs. ((2), (3), (10) and (11)), due to the path in the slabs j and $j+1$. The incidence and refraction angles (θ_{ij+2}, θ_{rj+2}) for the slab number $j+2$ can be calculated using the geometry of Fig. 4 as follows:

$$\theta_{ij+2} = \theta_{rj+1} \tag{17}$$

and

$$\theta_{rj+2} = \sin^{-1}\left[\frac{n_j}{n_{j+2}}\cos(\theta_{ij} - \theta_{rj})\right] \tag{18}$$

The beam will emerge at distance x_{ej+2}, which is given by the following equation:

$$x_{ej+2} = r\sin(\beta_{j+2}) \tag{19}$$

where

$$\beta_{j+2} = (\theta_{ej+2} + \theta_{rj+2}) - \frac{\pi}{2} \tag{20}$$

and

$$\theta_{ej+2} = \sin^{-1}\left(\frac{\mathrm{ON}_{j+2}}{r}\right) \tag{21}$$

The distance x_{j+2} is given by:

$$x_{j+2} = r - (j+1)a \tag{22}$$

As a result of the beam passing through the fibre slabs (j, $j+1$, $j+2$), the optical path difference will be given by the following equation:

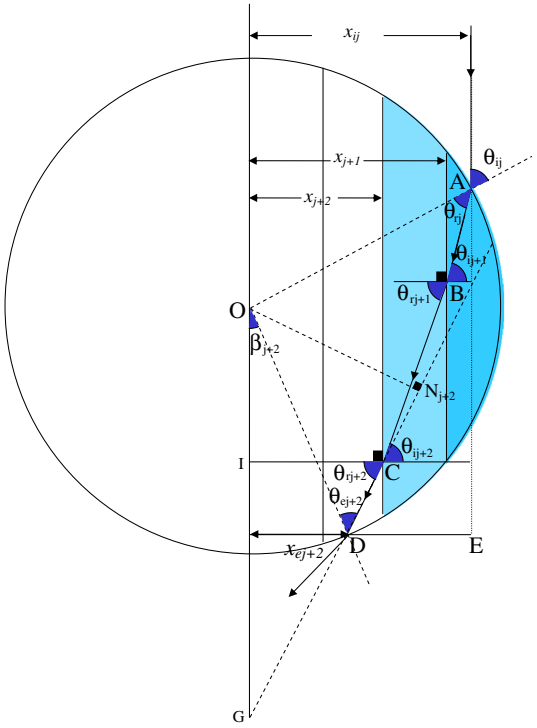

Fig. 4. The ray tracing across three slabs j, $j+1$, $j+2$.

$$\frac{\lambda Z_{jj+2}}{2h} = \left[n_j \frac{x_{ij} - x_{j+1}}{\sin}(\theta_{ij} - \theta_{rj}) + n_{j+1} \frac{x_{j+1} - x_{j+2}}{\cos(\theta_{rj+1})} + n_{j+2} \frac{x_{j+2} - x_{ej+2}}{\cos(\theta_{rj+2})} \right] - n_{\mathrm{L}} \left[\frac{x_{ij} - x_{j+1}}{\tan(\theta_{ij} - \theta_{rj})} + [(x_{j+1} - x_{j+2}) \tan \theta_{rj+1}] + [(x_{j+2} - x_{ej+2}) \tan \theta_{rj+2}] \right] \quad (23)$$

where Z_{jj+2} is the shift due to the path through the three slabs.

2.4. The refraction through k slabs

We can use the above derived relations to obtain recurrence relations to calculate the angles, distances and optical path difference due to the path of the incident light beam through k slabs. The incident beam will strike the fibre at the slab number j and will leave it from the slab number $j+k-1$. Now we can represent the recurrence relation, which describes the optical path difference in this case.

$$\frac{\lambda Z_{jj+k-1}}{2h} = \left[n_j \frac{x_{ij} - x_{j+1}}{\sin(\theta_{ij} - \theta_{rj})} + \sum_{l=j+1}^{j+k-2} n_l \frac{x_l - x_{l+1}}{\cos(\theta_{rl})} + n_{j+k-1} \frac{x_{j+k-1} - x_{ej+k-1}}{\cos(\theta_{rj+k-1})} \right] - n_{\mathrm{L}} \left[\frac{x_{ij} - x_{j+1}}{\tan(\theta_{ij} - \theta_{rj})} + \sum_{l=j+1}^{j+k-2} [(x_l - x_{l+1}) \tan \theta_{rl}] + \left[(x_{j+k-1} - x_{ej+k-1}) \tan \theta_{rj+k-1} \right] \right] \quad (24)$$

where Z_{jj+k-1} is the shift corresponding to the refraction of the incident light beam through k slabs and $l = j+1$, $j+2 \ldots j+k-2$. The above recurrence relation satisfies all values for $k = 2, 3 \ldots$ etc. The first and third terms are not under the summations of optical paths across the fibre and the liquid, because the beam enter the fibre slab number j at the curved surface of it and emerge the fibre slab number $J+k-1$ from the curved interface. The summations express the optical paths across the slabs, which the beam strikes and refracts through its parallel surfaces. The angles and distances state in the above recurrence relation can be expressed as:

$$\theta_{il+1} = \theta_{rl} \quad (25)$$

$$\theta_{rl} = \sin^{-1} \left[\frac{n_j}{n_l} \cos(\theta_{ij} - \theta_{rj}) \right] \quad (26)$$

and

$$x_l = r - (l-1)a \quad (27)$$

The beam will emerge at distance x_{el}, which is given by;

$$x_{el} = r \sin \beta_l \quad (28)$$

where

$$\beta_l = (\theta_{el} + \theta_{rl}) - \frac{\pi}{2} \quad (29)$$

And the emergence angle will be given by:

$$\theta_{el} = \sin^{-1} \left(\frac{\mathrm{ON}_l}{r} \right) \quad (30)$$

In the last case, we describe the refraction through multi-slabs of bent optical fibre cladding.

3. Experimental technique

The Fizeau interferometer in transmission is very sensitive and accurate multiple-beam interference based technique. Fig. 5a illustrates the schematic diagram of this interferometer. The wedge interferometer containing the bent optical fibre, which is immersed in a suitable liquid, is shown in Fig. 5b. The sharp interference pattern perpendicular to the fibre is obtained by adjusting the wedge angle and the gap thickness between the two optical flats. CCD camera attached to the microscope to capture the produced microinterferogram. The CCD connects to a PC through a

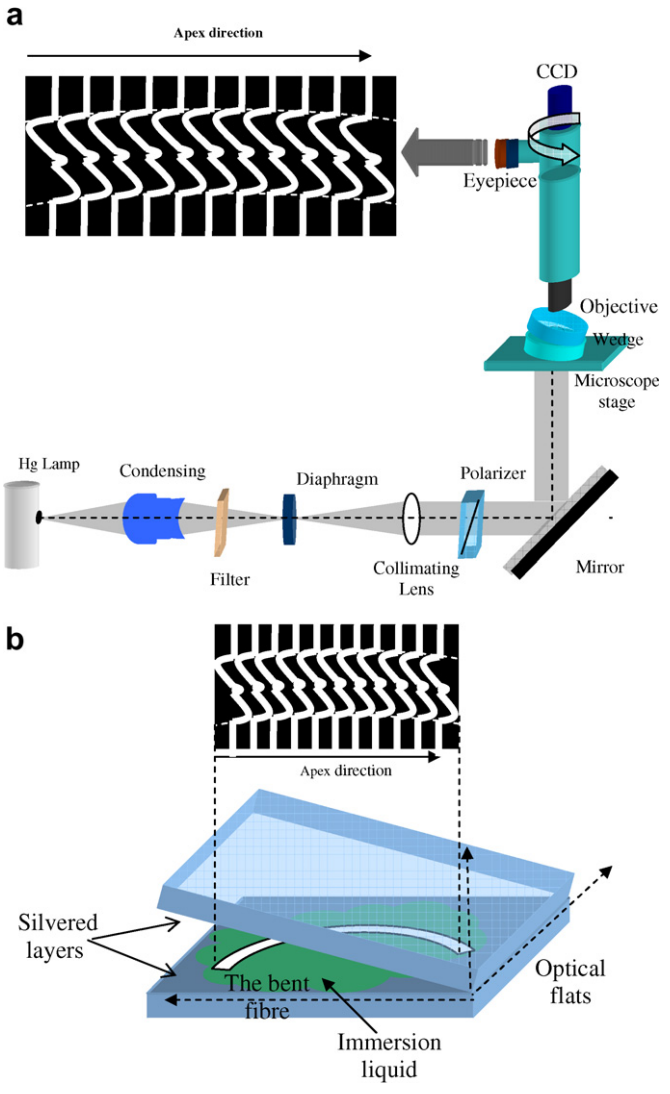

Fig. 5. The schematic diagrams of (a) Fizeau technique (b) the wedge interferometer.

frame grabber. Using CCD camera and frame grabber, the microinterferogram is transferred to the computer. Then the microinterferograms are analyzed using one dimension Fourier's transform [23]. Using a prepared program the refractive index profile and other optical parameters are calculated.

4. Experimental results and discussion

Multiple-beam Fizeau interferometer in transmission is used to characterize the bent optical fibre. The obtained microinterferograms of multiple-beam Fizeau fringes for strain free isotropic optical fibre immersed in different liquids are given in Fig. 6. Fig. 6b illustrates the microinterferogram in the matching case ($n_L = n_{cladding}$) using monochromatic light of wavelength $\lambda = 546.1$ nm. In the mismatching case ($n_L \neq n_{cladding}$) the fringe shift inside the cladding will be negative when $n_L > n_{cladding}$ and it will be positive when $n_L < n_{cladding}$ as shown in Fig. 6a and c, respectively. A comparative study for the refractive index profile of the used bent free optical fibre are carried out using the suggested slab model and the other models [8,21].

The refractive index profile of bent free homogenous optical fibre cladding is calculated considering the refraction using the model when the beam passing across the cladding only [8]. Also, the Hamza et al. (1995) multilayer refraction model [21] is used to obtain the refractive index profile of this fibre cladding as well as the described new slab model. Fig. 7 shows the calculated refractive index profiles which calculated using the mentioned three models. The obtained refractive index profile for free bent optical fibre using our described model gets good agreement with that profiles calculated using the well known models [8,21]. So that, the new slab model is valid with good accuracy.

The optical fibre is bent circularly with radius $R = 15.05$ mm. The effect of the bending on the optical fibre cladding refractive index appears as deformation of the fringe shift inside it. The microinterferogram shown in Fig. 8a is obtained when a polarized light component vibrating parallel to the fibre optical axis is used. The fringe shift along the bent optical fibre will be negative in the extension region and it will be positive in the compression region.

Fig. 8b shows the microinterferogram of Fizeau fringes when using a polarized light component vibrating perpendicular to the fibre axis. One notes that, the fringe shift across the bent optical fibre is not affected by the bending at this polarization state. This means that the bent optical fibre refractive index $n^{\perp}$ in the direction perpendicular to the fibre axis remains unchanged through the bending. In other words, the cladding refractive index $n^{\perp}$ will be equal to the refractive index n_L of the matching liquid. The isotropic optical fibre becomes anisotropic due to the bending effect. Because of the bending, the refractive index $n^{\parallel}$ of the bent optical fibre will change in the parallel direction.

The multilayer refraction model [21] and the new slab model are used to calculate the refractive index profile of the bent optical fibre (at $R = 21.9$ mm) which is given in Fig. 9. The multilayer refraction model cannot be used in the bending case. This is due to the multilayer model is considering the fibre cross section consists of large number of

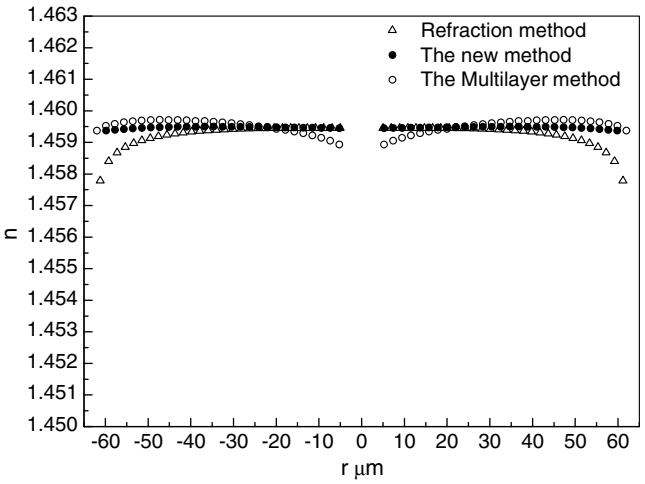

Fig. 7. The refractive index profiles calculated using the refraction method, multilayer method and the suggested method for the bent free optical fibre cladding.

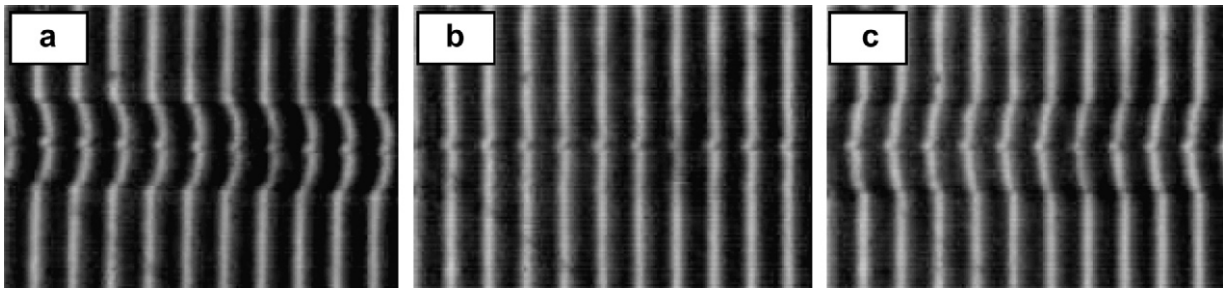

Fig. 6. Microinterferograms of multiple-beam Fizeau fringes for free strain optical fibre (a) $n_L = 1.4608$, (b) $n_L = 1.4595$ and (c) $n_L = 1.4585$ at $\lambda = 546.1$ nm.

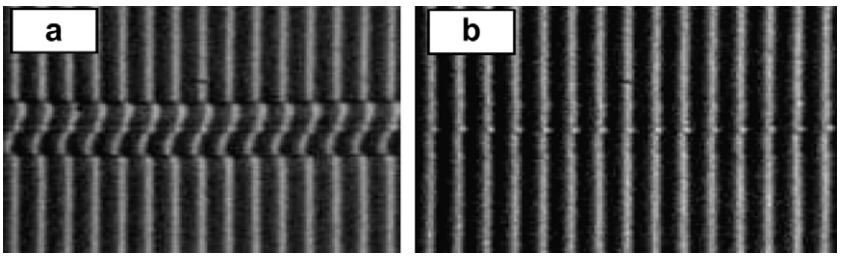

Fig. 8. The experimental microinterferograms of multiple-beam Fizeau fringes for the bent fibre at $R = 15.05$ mm, $n_L = 1.4595$ and $\lambda = 546.1$ nm, when using light beam vibrating (a) parallel and (b) perpendicular to the fibre axis.

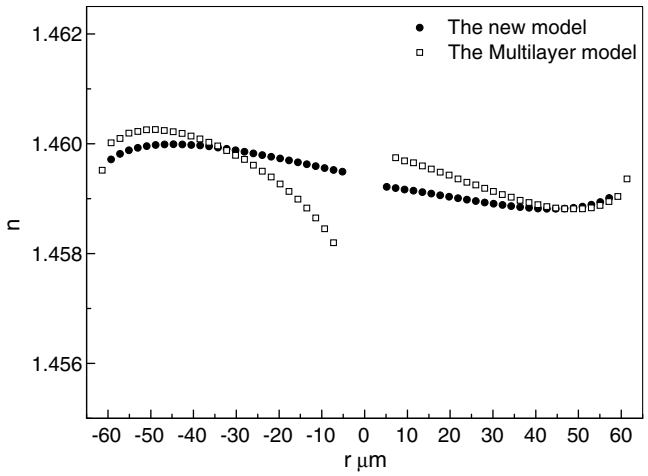

Fig. 9. The refractive index profiles for the bent optical fibre cladding calculated using the multilayer method and the suggested method at $R = 21.9$ mm.

circular zones. Every zone has a constant refractive index. Our new model (slabs) gives good prediction of the refractive index profile for the bent optical fibre cladding and more accurate results than when using the circular zone model [21].

A prepared image-processing program based on the Fourier transform mechanism used to obtain the contour lines of the fringe shifts. Fig. 10a–c shows the contour lines of the automated Fizeau fringes at different bent, when $R = 21.9$, 15.05 and 8.95 mm, respectively, and monochromatic light beam vibrating parallel to the fibre axis. The magnitude of the fringes shift is a function that decreases as the bending radius (R) increases and consequently the refractive index component in the parallel direction $n^{\|}$. In addition, the birefringence will increase as the bending radius decrease and vice versa. The automatic fringe analysis programme includes the calculation of the refractive index profile of the bent optical fibre cladding. This procedure based on the above described mathematical expressions which taking into consideration the refraction of the incident light beam by the liquid–fibre interface. Fig. 11 gives the refractive index profile $n^{\|}$ for the bent fibre with the refraction consideration at $R = 21.9$, 15.05 and 8.95 mm, respectively. The refractive index $n^{\|}$ of the bent optical fibre cladding increases in the compression region ($x < 0$) toward the fibre surface while it decreases in the extension region ($x > 0$). The matching liquid is used to obtain the mentioned microinterferograms at different radii of bending. Easily one can get the refractive index of the fibre $n^{\perp}$ which equals to the refractive index of the matching liquid ($n^{\perp} = 1.4595$ at $\lambda = 546.1$ nm). The induced birefringence ($\Delta n_{\text{induced}}$) was calculated with the refraction consideration and is given in Fig. 12 at $R = 21.9$, 15.05 and 8.95 mm, respectively. The induced birefringence has the same behavior as the refractive index ($n^{\|}$) profile along the bent fibre cladding diameter.

Bending of the fibre will affect the guidance parameters such as the numerical aperture N.A and the acceptance angle θ_m. The numerical aperture, which is important in the fields of applications and is given by $\text{N.A} = \sqrt{n_c^2 - (n^{11})^2}$. Where n_c is the refractive index of the core for the used single mode optical fibre. The N.A defined as the sine of the acceptance angle ($\text{N.A} = \sin\theta_m$).

Fig. 13 shows the calculated acceptance angle (θ_m) at different bending radii (at $R = 8.95$, 15.05 and 21.9 mm), respectively. This guiding parameter increases in the tension region and decreases in the compressed region.

The normalized index difference (Δ) can be calculated using the refractive indices values [1], $\Delta = \frac{n_c^2 - n_{cl}^2}{2\,n_c^2}$. The calculated refractive index of the core n_c for the used single mode optical fibre is $1.4624 \pm 1 \times 10^{-4}$. The refractive index of the bent free cladding n_{cl} is $1.4595 \pm 1 \times 10^{-4}$. Then, the calculated value of Δ is 0.2002%. This value is too closed to the standard value 0.2% [1] for such that single mode optical fibres.

To avoid large losses in the bent optical fibre the bending radius should be greater than a certain value. The model fields will be confined within and relatively close to the core under this condition [24] ($R \gg \frac{r_c V^2}{2\Delta}$). Using this condition and the values of (V, Δ and $r_c = 5$ μm) for the used fibre, the bending radius R can be calculated. Where V is the normalized frequency parameter, $V = 2.405$ [1]. Therefore, R must be greater than 7.1 mm.

In conclusion, the refractive index, the induced birefringence and the guidance parameters are dependent on the bending radius as well as the produced mechanical strain.

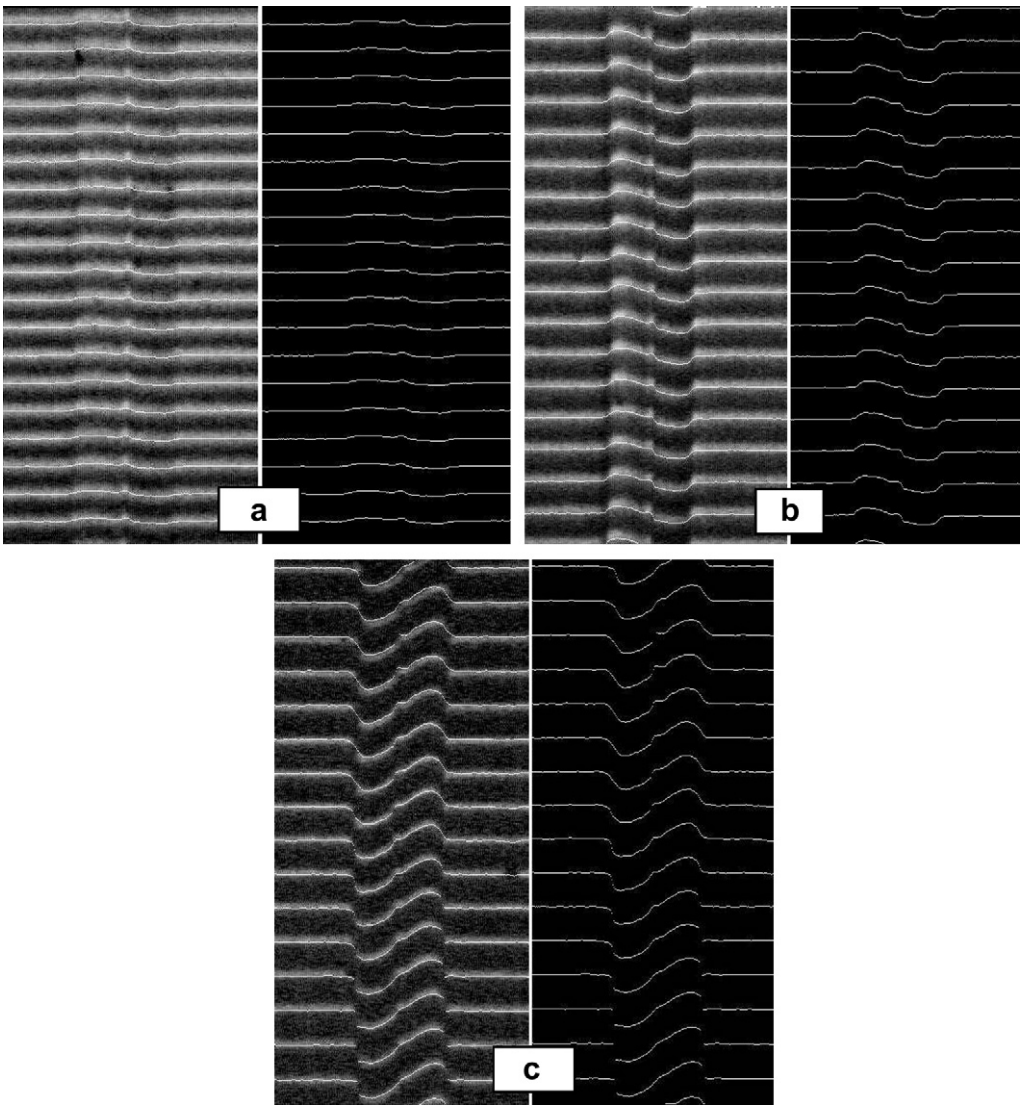

Fig. 10. The automated Fizeau fringes using a light beam vibrating parallel to the fibre axis at (a) $R = 21.9$, (b) $R = 15.05$ and (c) $R = 8.95$ mm, respectively.

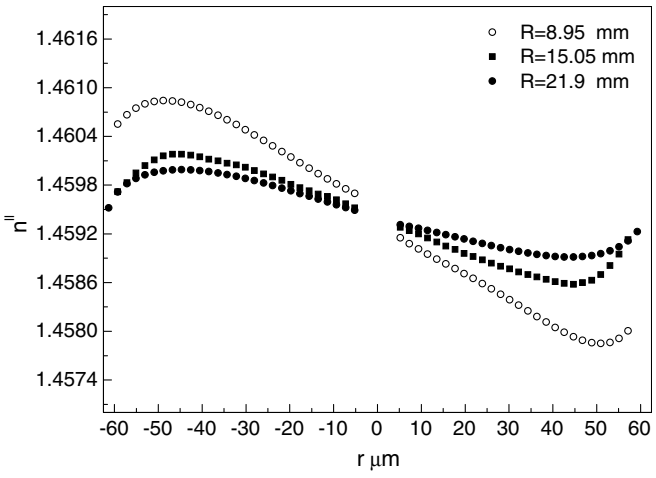

Fig. 11. The refractive indices ($n^{\parallel}$) profiles of the bent fibres cladding with the refraction considerations at $R = 21.9$, 15.05 and 8.95 mm.

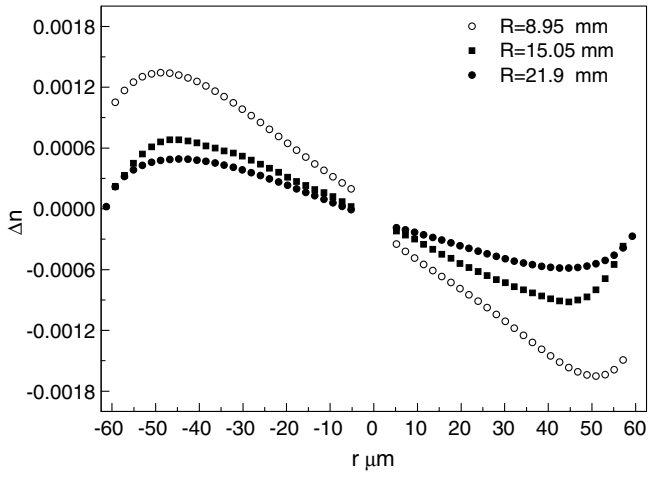

Fig. 12. The induced birefringences of the bent fibres cladding with the refraction consideration at $R = 21.9$, 15.05 and 8.95 mm.

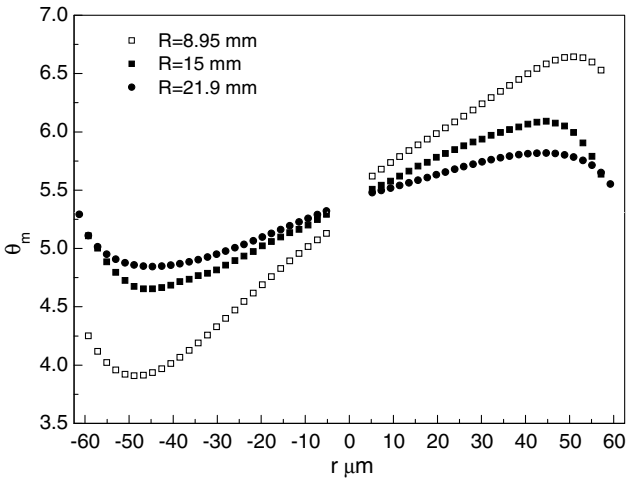

Fig. 13. The acceptance angle (θ_m) across the bent optical fibres cladding at $R = 8.95$, 15.05 and 21.9 mm.

5. Conclusion

The isotropic optical fibre material becomes anisotropic material under the effect of mechanical bending. The induced anisotropy in the bent optical fibre leads to the appearance of the optical birefringence. The zones model [21] does not predict the refractive index profile of the bent fibre. Other coworker deals with this problem neglecting the refraction of the incident beam by the fibre [19,25].

In this work, the automated multiple-beam Fizeau interferometer based on the Fourier transform fringe analysis technique is used to calculate the refractive indices, the induced birefringence and the guidance parameters of the bent optical fibre cladding at different bending radii. A new slab model considering the refraction of the incident beam through the liquid/fibre interface is the base of the calculations. The optical and guidance parameters across the bent optical fibre cladding regions (compression and extension) are calculated with high accuracy. The refractive indices taking refraction of the light beam into consideration are obtained as well as the induced birefringence. The bent radius is recommended to be greater than 7.1 mm to avoid model fields losses. The advantage of this technique is based on the refraction consideration as well as the aid of the prepared image processing programs. The computerized Fizeau interferometer helps one to save time and gets highly accurate results.

Acknowledgement

The authors would like to express their gratitude to Professor A.A. Hamza for his useful discussions.

References

[1] John A. Buck, Fundamentals of Optical Fibers, John Wiley & Sons, Inc. New York, 1995, p. 48.
[2] C.R. Hammond, S.R. Norman, Opt. Quant. Elect. 9 (1977) 399.
[3] R.C. Faust, Physical Methods of Investigation Textiles, Textile Book Pub. Inc. New York, 1959.
[4] M.J. Saunder, W.B. Gardner, Appl. Opt. 16 (1977) 2368.
[5] N. Barakat, A.A. Hamza, A.S. Ganied, Appl. Opt. 24 (1985) 4383.
[6] N. Barakat, A.A. Hamza, Interferometry of Fibrous Material, Adam Hilger, Bristol and New York, 1990, p. 55.
[7] T.Z.N. Sokkar, Opt. Commun. 35 (1991) 187.
[8] A.A. Hamza, T.Z.N. Sokkar, M.A. Mabrouk, A.M. Ghandar, W.A. Ramadan, Pure Appl. Opt. 3 (1994) 943.
[9] T.Z.N. Sokkar, M.A. Mabrouk, H.F. El-Bawab, J. Opt. A: Pure Appl. Opt. 1 (1999) 64.
[10] A.A. Hamza, T.Z.N. Sokkar, M.A. Mabrouk, M.A. El-Morsy, J. Appl. Poly. Sci. 77 (2000) 3099.
[11] A.A. Hamza, M.A. Mabrouk, W.A. Ramadan, H.H. Wahba, Opt. Lasers Eng. 42 (2004) 121.
[12] A.A. Hamza, A.E. Belal, T.Z.N. Sokkar, H.M. EL-Dessouky, M.A. Agour, Opt. Lasers Eng. 45 (2007) 145.
[13] Y. Hibino, F. Hanawa, M. Horiguchi, J. Appl. Phys. 65 (1989) 30.
[14] J. Zubia, J. Arrue, IEE Proc. Optoelectron. 144 (1997) 397.
[15] H. Tai, R. Rogowski, Opt. Fiber Tech. 8 (2002) 162.
[16] H. Vendeltorp-Pommer, J.H. Povlsen, Opt. Commun. 75 (1990) 25.
[17] J. Yamauchi, M. Ikegaya, H. Nakano, IEE Proc. J 139 (1992) 201.
[18] Y. Liu, L. Zhang, J.A.R. Williams, I. Bennion, Opt. Commun. 193 (2001) 69.
[19] F. El-Diasty, J. Opt. A: Pure Appl. Opt. 1 (1999) 197.
[20] Wong Chi Ming, Image Processing in Experimental Mechanics, Master of Philosophy, University of Hong Kong, 1993.
[21] A.A. Hamza, A.M. Ghander, T.Z.N. Sokkar, M.A. Mabrouk, W.A. Ramadan, Pure Appl. Opt. 4 (1995) 161.
[22] M. Born, E. Wolf, Principles of Optics, Cambridge University Press, Cambridge, 1999, p. 834.
[23] M.A. El-Morsy, T. Yatagai, A.A. Hamza, M.A. Mabrouk, T.Z.N. Sokkar, J. Appl. Polym. Sci. 85 (2002) 475.
[24] S.J. Garth, W.M. Henry, J.D. Love, Opt. Quant. Elect. 27 (1995) 15.
[25] F. El-Diasty, J. Opt. A: Pure Appl. Opt. 4 (2002) 575.